Theoretical and Experimental Studies of the Spin Trapping of Inorganic Radicals by 5,5-Dimethyl-1-Pyrroline *N*-Oxide (DMPO). 1. Carbon Dioxide Radical Anion

Frederick A. Villamena,*,† Edward J. Locigno,† Antal Rockenbauer,§ Christopher M. Hadad,*,‡ and Jay L. Zweier*,†

Center for Biomedical EPR Spectroscopy and Imaging, The Davis Heart and Lung Research Institute, and the Division of Cardiovascular Medicine, Department of Internal Medicine, College of Medicine and the Department of Chemistry, The Ohio State University, Columbus, Ohio 43210, and Chemical Research Center, Institute for Structural Chemistry, H-1025 Budapest, Pusztaszeri ut 59, Hungary

Received: July 31, 2006; In Final Form: September 27, 2006

The carbon dioxide radical anion ($CO_2^{\bullet-}$) is known to be generated in vivo through various chemical and biochemical pathways. Electron paramagnetic resonance (EPR) spin trapping with the commonly used spin trap, 5,5-dimethyl-1-pyrroline *N*-oxide (DMPO), has been employed in the detection of $CO_2^{\bullet-}$. The thermodynamics of $CO_2^{\bullet-}$ addition to DMPO was predicted using density functional theory (DFT) at the B3LYP/6-31+G**//B3LYP/6-31G* and B3LYP/6-311+G* levels with the polarizable continuum model (PCM) to simulate the effect of the bulk dielectric effect of water on the calculated energetics. Three possible products of $CO_2^{\bullet-}$ addition to DMPO were predicted: (1) a carboxylate adduct, (2) pyrroline-alcohol and (3) DMPO−OH. Experimentally, UV photolysis of H_2O_2 in the presence of sodium formate ($NaHCO_2$) and DMPO gave an EPR spectrum characteristic of a C-centered carboxylate adduct and is consistent with the theoretically derived hyperfine coupling constants (hfcc). The pK_a of the carboxylate adduct was estimated computationally to be 6.4. The mode of $CO_2^{\bullet-}$ addition to DMPO is predicted to be governed predominantly by the spin (density) population on the radical, whereas electrostatic effects are not the dominant factor for the formation of the persistent adduct. The thermodynamic behavior of $CO_2^{\bullet-}$ in the aqueous phase is predicted to be similar to that of mercapto radical ($^{\bullet}SH$), indicating that formation of $CO_2^{\bullet-}$ in biological systems may have an important role in the initiation of oxidative damage in cells.

Introduction

Reactive oxygen species (ROS) have been implicated in the toxicology of various xenobiotics and in the pathogenesis of various diseases.[1−4] Since inorganic anions are ubiquitous in most biological and environmental systems, the interaction of these species with ROS such as hydroxyl radical ($HO^{\bullet}$) may lead to the production of highly oxidizing or reducing radical species that can be detrimental to cell viability. Moreover, from an analytical perspective, production of these ROS derived inorganic radical species may lead to an erroneous interpretation of electron paramagnetic resonance (EPR) spectra observed from nitrone spin traps.

EPR spin trapping[5−11] has been an indispensable tool in the detection of oxygen radical species using the nitrone 5,5-dimethyl-1-pyrroline *N*-oxide (DMPO),[12−18] which has been widely employed as a spin trap in the detection of transient radicals in chemical or biological systems. For example, two distinct spectra could be obtained from DMPO−OH and DMPO−OOH adducts arising from the addition of $HO^{\bullet}$ and $O_2^{\bullet-}$ to DMPO, respectively.[19] This "fingerprinting" of radicals can be utilized to identify free radicals unambiguously, thus providing a spectral "snapshot" of the radical being investigated (Scheme 1).

SCHEME 1

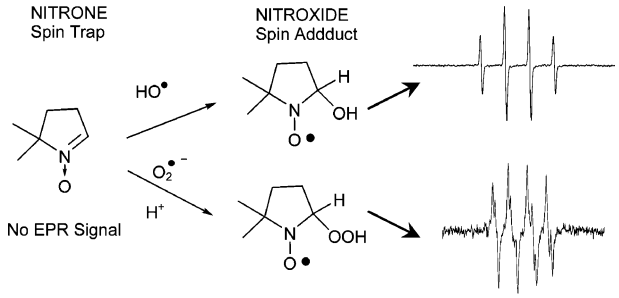

In spite of this unique feature of spin trapping, there are still major limitations in its application, and one of them is the accurate interpretation of the generated EPR spectra. Since spin trapping is often applied to complex biological or chemical systems, it is important to have a clear understanding of the nature of the adducts formed from various radicals which would be present in a complex mixture. Spin-trapping experiments performed in the presence of inorganic anions may lead to secondary radical adduct formation, so that knowledge of the formed inorganic radical anion adduct is important for the accurate interpretation of certain fundamental chemical and biological processes. It is therefore critical to identify and examine the nature of these anion-derived radical species formed under spin-trapping conditions.

The role of carbon dioxide radical anion ($CO_2^{\bullet-}$) formation in acute sodium formate poisoning has been reported.[20] This radical is also generated as a metabolic product of CCl_4 in rat liver microsomes.[21,22] There were attempts to characterize $CO_2^{\bullet-}$

* To whom correspondence should be addressed. (F.A.V.) E-mail: Frederick.Villamena@osumc.edu. Fax: (614)-292-8454. (C.M.H.) E-mail: hadad.1@osu.edu.Fax: (614)-292-1685.(J.L.Z.)E-mail: Jay.Zweier@osumc.edu. Fax: (614)-247-7799.

† The Davis Heart and Lung Research Institute, and the Department of Internal Medicine, The Ohio State University.

‡ Department of Chemistry, The Ohio State University.

§ Institute for Structural Chemistry.

10.1021/jp064892m CCC: $33.50
Published on Web 11/21/2006

by EPR spin trapping using DMPO as a spin trap, but the nature of the radical adducts formed was not well understood.[23−26] It is therefore important to determine the spin-trapping characteristic of $CO_2^{\bullet-}$ in order to accurately interpret the resulting EPR spectra during their formation in chemical and biological systems. This study will characterize the spin-trapping process by 5,5-dimethyl-1-pyrroline *N*-oxide (DMPO) of $CO_2^{\bullet-}$ generated from UV photolysis of $NaHCO_2$[27] in the presence of H_2O_2. Various modes of radical addition and the stabilities of spin adducts formed will be theoretically and experimentally assessed.

Experimental Methods

General Computational Methods. Density functional theory[28,29] was applied in this study to determine the optimized geometry, vibrational frequencies, and single-point energy of all stationary points.[30−33] The effect of solvation on the gaseous phase calculations was also investigated using the polarizable continuum model (PCM).[34−38] All calculations were performed using Gaussian 03[39] at the Ohio Supercomputer Center. Single-point energies were obtained at the B3LYP/6-31+G** level based on the optimized B3LYP/6-31G* geometries, and the B3LYP/6-31+G**//B3LYP/6-31G* wave functions were used for natural population analyses (NPA).[40] These basis set calculations used the standard six Cartesian d functions. Geometry optimization with diffuse functions at the B3LYP/6-311+G* level of theory was performed to account for the negative charge character of the species being investigated using five (pure) d polarization functions for these calculations. Vibrational frequency analyses (B3LYP/6-31G*) for each of the stationary points for DMPO and its $CO_2^{\bullet-}$ adducts yielded only real vibrational frequencies. A scaling factor of 0.9806 was used for the zero-point vibrational energy (ZPE) corrections with the B3LYP/6-31G* and the B3LYP/6-311+G* levels of theory.[41] Spin contamination for all of the stationary point of the radical structures was negligible, i.e., $0.75 < \langle S^2 \rangle < 0.77$.

Calculation of Isotropic Hyperfine Coupling Constants (hfcc). The prediction of hfcc of the nitrogen atom in simple nitroxides was demonstrated in several landmark works.[42−45] Based on these previous studies,[42−45] we employed similar models in the prediction of hfcc's of the nitrogen, β-hydrogen, and γ-hydrogens of DMPO−O_2H, and a discussion of the comparative study of calculated hfcc for DMPO−O_2H optimized at the B3LYP density functional and basis sets, 6-31+G**, 6-31G*, EPR-II and EPR-III,[46] and the core-valence correlation-consistent cc-pCVDZ[47] in the gas and aqueous phases can be found on pages S13−S18 of the Supporting Information of our previous paper.[48] Also, in the same paper,[48] the hybrid PBE0 functional and EPR-II basis set was found[45] to yield accurate a_N values in simple nitroxides and was also employed in the calculation of hfcc for DMPO−O_2H. Although the levels of theory mentioned above gave accurate a_N for 2,2,5,5-substituted pyrrolidine nitroxides, the calculated hfcc's for DMPO−O_2H using the same levels of theory gave errors (theoretical hfcc versus experimental hfcc) comparable to that predicted at B3LYP/6-31+G(d,p)//B3LYP/6-31G(d). Hence, in this study, the a_N, $a_{\beta-H}$, and $a_{\gamma-H}$ for all of the spin adducts were only calculated at the B3LYP/6-31+G(d,p)//B3LYP/6-31G(d) level.

EPR Measurements. EPR measurements were carried out on an X-band spectrometer with HS resonator at room temperature. General instrument settings are as follows unless otherwise noted: microwave power, 10 mW; modulation amplitude, 0.5 G; receiver gain, $3.17-3.56 \times 10^5$; time constant, 82 ms; time sweep, 42 s. EPR measurements were carried out on an X-band spectrometer with HS resonator at room temperature. Simulation of spectra was performed using the program developed by Rockenbauer, et al.[49]

Spin Trapping Studies. DMPO (99.9%), $NaHCO_2$ (99.5%), 30% H_2O_2 in water, and 80% $H_2{}^{17}O_2$-20% $H_2{}^{16}O_2$ were obtained commercially. All solutions were prepared using deoxygenated, double-distilled water. The total volume of each solution used for the EPR measurement was 50 μL and was loaded into a 50 μL quartz micropipette. The carbon dioxide radical anion was generated from irradiation[27] with a low-pressure mercury vapor lamp at 254 nm wavelength of 100 mM aqueous solutions of $NaHCO_2$ in the presence of 25−50 mM DMPO, and 100 μM H_2O_2 (or 100 μM 80% $H_2{}^{17}O_2$-20% $H_2{}^{16}O_2$) EPR spectra were acquired over the course of 10 min.

Results and Discussion

Carboxyl Radical Anion ($CO_2^{\bullet-}$) Adducts. *Electronic, Structural, and Thermodynamic Analysis.* Theoretical analysis of the $CO_2^{\bullet-}$ was carried out at the B3LYP/6-31+G**//B3LYP/6-31G* level and shows a bent geometry with C_{2v} symmetry. The charge density distribution of $CO_2^{\bullet-}$ from an NPA reveals negative character on the 2 O atoms (−0.76 e) and a positive charge on the C atom (+0.52 e). Calculated C−O bond lengths in $CO_2^{\bullet-}$ gave a bond distance of 1.25 Å consistent with the experimental C−O bond distances of 1.26 ± 0.01 Å in carboxylates.[50] Spin (densities) populations indicate a 68% electron delocalization on the C atom, consistent with the charge density calculations.

For the addition of $CO_2^{\bullet-}$ to DMPO, three products were theoretically predicted (i.e., DMPO−CO_2, a C-centered radical adduct, and two O-centered adducts, DMP−OCO_2 and DMPO−OCO; Figure 1). Calculated bond angles and distances in DMPO and the corresponding nitroxyl CO_2-adduct DMPO−CO_2 are consistent with experimental C−N and N−O bond distances in analogous nitrones and nitroxyl compounds.[51−53] However, DMPO−OCO showed a much longer C5-N bond distance of 1.55 Å compared to DMPO−CO_2 and DMPO−OCO_2.

The formation of the DMPO−CO_2 adduct is exoergic by $\Delta G_{298K,aq} = -12.1$ kcal/mol in the aqueous phase (reaction A, Scheme 2). The calculated $C_{ring}-C_{CO2}$ bond distance of 1.60 Å and the $C_{CO2}-O_{CO2}$ bond distance of 1.26 Å for DMPO−CO_2 is close to the X-ray crystallographic values of 1.51−1.52 and 1.22−1.30 Å, respectively, found in Cu(II) 3-carbamoyl-2,2,3-trimethylcyclopentane-1-carboxylate[54] and Mo(VI) amino acid complexes.[55] The calculated N−O and C−N bond distances are 1.49 and 1.46 Å, respectively, and the 48% (N) and 46% (O) spin populations for the nitroxyl moiety in DMPO−CO_2 indicate the formation of a carboxylate-pyrroline-*N*-oxyl radical anion.

Optimization of the O-centered adduct (DMPO−OCO) yielded two final structures, DMP−OCO_2 and DMPO−OCO (Figure 1 and Scheme 2). An aminyl radical, DMP−OCO_2, was formed via the intramolecular nitronyl-O atom abstraction by the carbonyl-C moiety. The calculated free energy of reaction for the formation of DMP−OCO_2 in the aqueous phase (i.e., reaction B + C; Scheme 2 and Table 1), is $\Delta G_{298K,aq} = -21.4$ kcal/mol, which is 9.3 and 11.1 kcal/mol more exoergic than the formation of DMPO−CO_2 and DMPO−OCO, respectively. Examination of the radical character of DMP−OCO_2 indicates that 87.9% of the unpaired electron is localized on the aminyl-

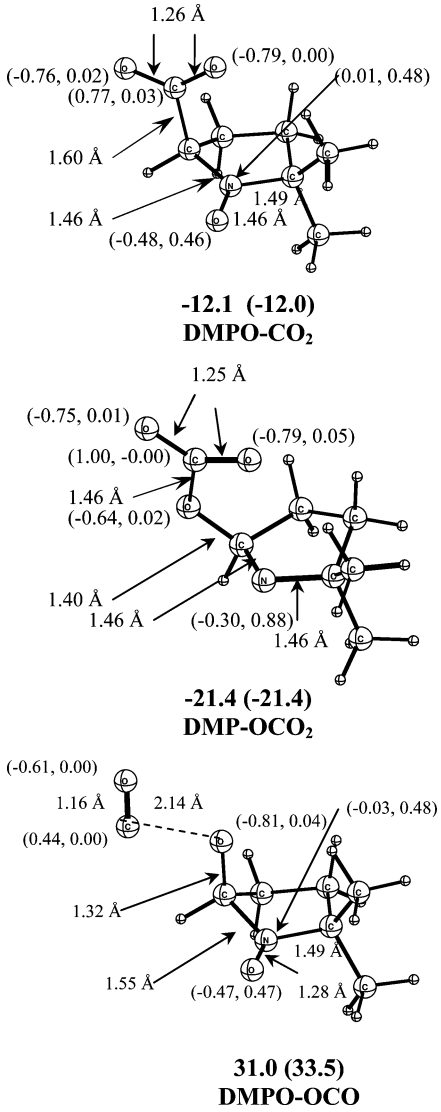

Figure 1. Bond distances, charge and spin density population (in parentheses) of various products arising from the addition of $CO_2^{\bullet-}$ addition to DMPO at the B3LYP/6-31+G**//B3LYP/6-31G* level. Aqueous phase reaction free energies ($\Delta G_{298K,aq}$ in kcal/mol) at the PCM/B3LYP/6-311+G* level. In parentheses, $\Delta G_{298K,aq}$ are presented at the PCM/B3LYP/6-31+G**//B3LYP/6-31G* level in kcal/mol.

N, while 4.2% is localized on the β-H (the highest among all of the H atoms in the molecule). Aminyl radicals are the most elementary class of nitrogen-centered organic radicals[56] and are highly reactive, short-lived intermediates considered to play an important role in chemical[57] and biological processes.[58] The most common mechanism for the formation of aminyl radicals is via thermal or photochemically induced homolytic bond cleavage of the N−H bond or by nitrogen oxidation.[59−61] Recently, aminyl ($^{\bullet}NR_2$) radicals have been stabilized by metal coordination as reported by Buettner et al.,[62] and EPR along with DFT studies show a spin density distribution of 56% on the aminyl-N and 36% on the Rh(I). This high value of the spin density distribution on the aminyl-N in the Rh(I)−aminyl complex is consistent with the spin distribution predicted for the aminyl-N in DMP−OCO_2 of 87.9%. Thus far, our study shows the first theoretical evidence for the formation of aminyl radicals from a nitroxide. However, due to the high reactivity of the DMP−OCO_2 intermediate, its possible fate in solution is the formation of the pyrroline−carbonate (DMPH−OCO_2^-) via subsequent H-atom abstraction (reaction D, Scheme 2). An

SCHEME 2

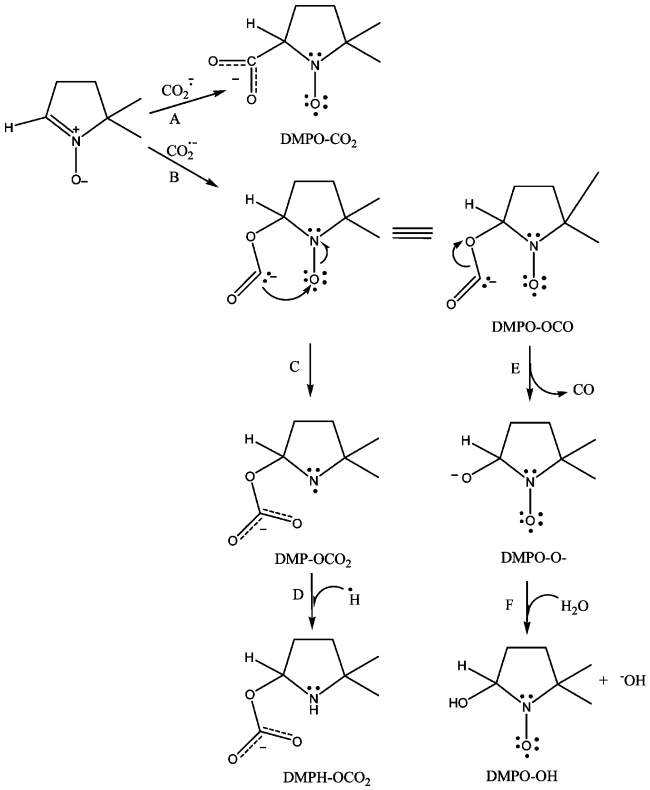

TABLE 1. Aqueous Phase Reaction Enthalpies ($\Delta H_{298K,aq}$) and Free Energies ($\Delta G_{298K,aq}$) for Various Modes of $CO_2^{\bullet-}$ Addition to DMPO at the PCM/B3LYP/6-311+G* Level in kcal/mol

entry	$\Delta H_{298K,aq}$	$\Delta G_{298K,aq}$
$CO_2^{\bullet-}$ + DMPO		
DMPO−CO_2	−23.7	−12.1
DMP−OCO_2	−33.4	−21.4
DMPO−OCO	22.1	31.0
Scheme 2		
A	−23.7	−12.1
B+C	−33.4	−21.4
D	16.5	24.9
B+E	−1.5	−10.0
F	6.7	7.5

experimental evaluation of aminyl radical formation will be presented below.

Analysis of the optimized structure of DMPO−OCO reveals two different C−O bond distances for the carboxylate group (i.e., 2.14 Å for $C_{CO2}-O_{ring}$ and 1.16 Å for $C_{CO2}-O_{CO2}$; Figure 1). The calculated C−O bond distance of 1.16 Å for one of the carboxylate C−O bonds is close to that observed for the experimentally observed C−O bond distance for carbon monoxide of 1.13 Å.[50] This difference in C−O bond distances is indicative of a heterolytic C−O bond cleavage to give carbon monoxide (C≡O) and pyrroline-*N*-oxyl alkoxide, DMPO−O^-. Vibrational analysis of the DMPO−OCO optimized structure yields no imaginary vibrational frequencies but did yield a small vibrational frequency of 29.8 cm^{-1}, indicative of a weak van der Waals interaction between the C≡O and DMPO−O^-. This suggests that DMPO−OCO is a local minimum on the potential energy surface but may exist in a shallow well. The NPA atomic charge on the carboxylate-O attached to the ring is −0.81 e which is close to the calculated charge of −0.97 e for O in CH_3O^- at the same level of theory, further confirming the formation of an alkoxide, DMPO−O^-. Although the eventual formation of DMPO−OH via proton abstraction by DMPO−

O^- from H_2O is endoergic by 7.5 kcal/mol ($\Delta G_{298K,aq}$; reaction F, Scheme 2), the overall free energy of reaction leading to the formation of DMPO−OH is exoergic with $\Delta G_{298K,aq} = -2.5$ kcal/mol. However, the formation of DMPO−OH from DMPO−OCO is the least thermodynamically favored product, as compared to the formation of DMPO−CO_2 or DMP−OCO_2.

We previously demonstrated that HO$^\bullet$ addition to nitrones is highly exoergic in the aqueous phase ($\Delta G_{rxn,298K} \sim -39$ kcal/mol),[14,63] and experimentally, the rate of HO$^\bullet$ addition to nitrones is very fast with second-order rate constants on the order of 10^9 M^{-1} s^{-1}.[64] However, we also theoretically and experimentally demonstrated[14,64] that HO$^\bullet$ addition to nitrones is more favored in nitrones bearing some positive charge on the nitronyl-C, the site of radical addition; hence, the nature of HO$^\bullet$ addition to nitrones is somewhat nucleophilic in nature. The character of HO$^\bullet$ addition to nitrones could be due to the negative charge density of −0.45 e and 100% spin distribution on the O atom of the HO$^\bullet$.[14] Although $CO_2^{\bullet-}$ also exhibits negative charge on its oxygens (i.e., −0.76 e), 68% of the spin density is localized mostly on its C atom. Based on the preference of $CO_2^{\bullet-}$ to form a C-centered adduct with DMPO by ∼41 kcal/mol compared to the formation of an O-centered adduct, it can be inferred that the nature of $CO_2^{\bullet-}$ addition to DMPO is mostly governed by its spin population rather than the charge characteristics of its atoms.

EPR Spin Trapping. Experimentally, the $CO_2^{\bullet-}$ radical anion was generated by UV photolysis (254 nm) in an aqueous H_2O_2 solution containing sodium formate ($NaHCO_2$) and DMPO. Figure 2 shows the resulting EPR spectrum for the addition of $CO_2^{\bullet-}$ to DMPO, revealing only the formation of a major sextet signal (99%) with $a_N = 15.74$ G and $a_{\beta-H} = 18.74$ G. The formation of the DMPO−CO_2 adduct from the 1-electron oxidation of HCO_2^- by HO$^\bullet$ was further confirmed by using $H_2{}^{17}O_2/H_2{}^{16}O_2$ (Figure 2b). A UV-irradiated solution of DMPO, either in the presence of $H_2{}^{17}O_2/H_2{}^{16}O_2$ or $H_2{}^{16}O_2$, gave an EPR spectrum with $a_N = 15.74$ G and $a_{\beta-H} = 18.74$ G (Table 2 and Figure 2), which is different from the hfcc's that would have arisen from DMPO−^{16}OH or DMPO−^{17}OH adducts. These results indicate the absence of any adducts originating from HO$^\bullet$ radicals.

The calculated isotropic hyperfine coupling constants (hfccs) of various products for the $CO_2^{\bullet-}$ addition to DMPO are shown in Table 2. Gas-phase hfcc calculations at the B3LYP/6-31+G**//B3LYP/6-31G* level of theory have been employed previously[65] to predict the a_N and $a_{\beta-H}$ of DMPO−OH and DMPO−O_2H adducts. From that study, the predicted gas-phase a_N values are 11.69 G for DMPO−OH and 11.87 G for DMPO−O_2H, an underestimation of 3.31 and 2.43 G, respectively, compared to their experimental hfcc values. Also, the gas-phase $a_{\beta-H}$ of 5.92 G for DMPO−OH and 6.60 G for DMPO−O_2H were also underestimated by 8.83 and 5.1 G, respectively. However, using more realistic computational models, which account for the explicit interaction of water as well as the bulk dielectric effect of water, can greatly improve the a_N and $a_{\beta-H}$ as has been previously demonstrated for DMPO−OH and DMPO−O_2H (see Table 2).[37,65] However, in this study, due to the high computational cost associated with using such models, direct calculation of the hfcc values in the gas phase was used. It follows, then, that the predicted gas-phase hfcc's for DMPO−CO_2 should give an underestimated a_N and $a_{\beta-H}$ in the range predicted for DMPO−OH and DMPO−O_2H at the B3LYP/6-31+G**//B3LYP/6-31G* level of theory. The predicted hfcc values for DMPO−CO_2 are $a_N =$ 11.37 G and $a_{\beta-H} = 8.52$ G, which are underestimated by 4.37 and 10.22 G, respectively, relative to the experimental values of $a_N = 15.74$ G and $a_{\beta-H} = 18.74$ G. These predicted hfcc values for DMPO−CO_2 are reasonable values on the basis of what have been predicted for DMPO−OH and DMPO−O_2H. As shown in Table 2, the DMP−OCO_2 product gave unreasonable overestimated hfcc values of $a_N = 15.36$ G and $a_{\beta-H} =$ 37.14 G, whereas DMPO−OCO gave underestimated values of $a_N = 13.30$ G and a significantly low $a_{\beta-H}$ of 0.43 G.

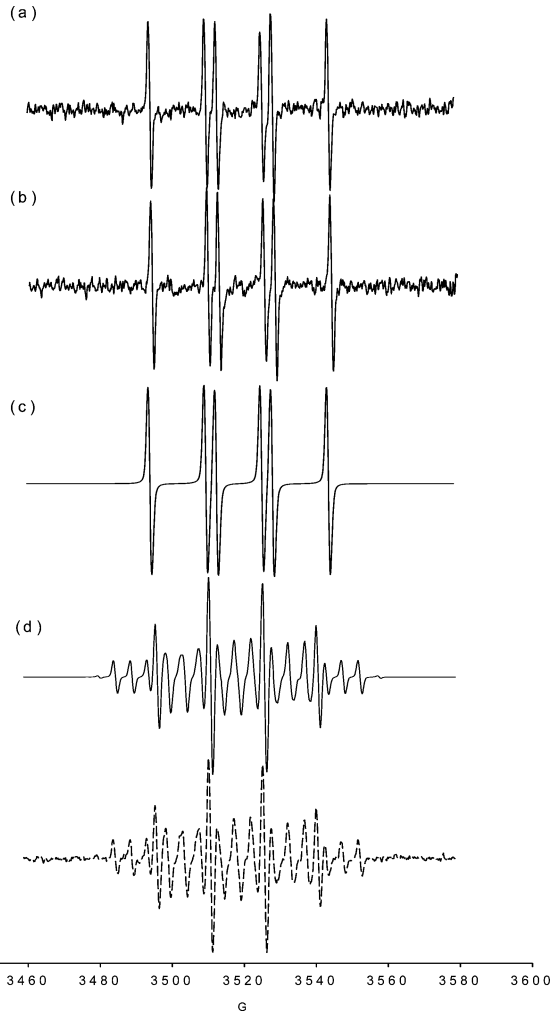

Figure 2. X-band EPR spectrum of the carbon dioxide radical ($CO_2^{\bullet-}$) addition to DMPO by UV photolysis of 100 mM $NaHCO_2$ in the presence of 50 mM DMPO and (a) 100 μM H_2O_2-^{16}O; (b) 100 μM (80%/20%) $H_2{}^{17}O_2$/ $H_2{}^{16}O_2$; (c) simulated spectrum; (d) UV photolysis of 50 mM DMPO and 100 μM (80%/20%) $H_2{}^{17}O_2/H_2{}^{16}O_2$ alone and simulated spectrum (dotted line). See the Experimental Section for the EPR parameters used.

However, inferences derived from the calculated hfcc may seem disputable due to their still relatively high error compared to the experimental values. Therefore, results from the EPR spin trapping experiments using isotopically enriched $H_2{}^{17}O_2$ which did not yield a spectrum typical of DMPO−^{17}OH (as described above) unequivocally suggest that the major peak arising from the $CO_2^{\bullet-}$ addition to DMPO is most probably that of the DMPO−CO_2 adduct.

To experimentally test if DMPH−OCO_2^- is formed, $NaHCO_2$ (100 mM) was irradiated in the presence of DMPO (50 mM) and H_2O_2 (58 mM), and product analyses using GC-MS as well as thin layer chromatography were carried out. Extraction of the reaction mixture with $CHCl_3$ and GC-MS analysis of the $CHCl_3$ extract gave no evidence of DMPH−OCO_2^- formation. Moreover, thin layer chromatography of the aqueous reaction

TABLE 2. Calculated Isotropic Hyperfine Coupling Constants (hfcc's) in Gas and Aqueous Phases at the B3LYP/6-31+G of N, β-H, and γ-H[a] of Various DMPO Spin Adducts Using the B3LYP/6-31G* Optimized Geometry**

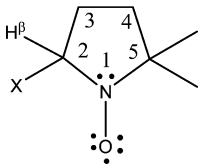

	isotropic hyperfine splitting constants (G)		
adduct	nitronyl-N	β-H	γ-H[b]
	Theoretical		
DMPO−CO_2	11.37	8.52	
DMPO−CO_2H	11.89	20.24	
DMP−OCO_2	15.36	37.14	
DMPO−OCO	13.30	0.43	1.86; 1.12
DMPO−OH	11.69	5.92	
DMPO−OH•$(H_2O)_2$[a]	12.89	9.38	
DMPO−O_2H	11.87	6.60	
DMPO−O_2H•$(H_2O)_2$[a]	11.76	13.62	
	Experimental		
$CO_2^{\bullet-}$ + DMPO	15.74	18.74	
DMPO−OH[c]	15.00	14.75	
DMPO−^{17}OH[d]	14.98	14.72	^{17}O = 4.65 ^{13}C(2) = 5.3 ^{13}C(2) = 7.0 G
DMPO−O_2H[d]	14.3	11.7	1.25

[a] Predicted hfcc with 2 explicit water molecules at the PCM/B3LYP/6-31+G** level. The Δa_x (defined as $a_{aq} - a_{gas}$) for the effect of solvation on hfcc for DMPO−OH are $\Delta a_N = 1.20$ G and $\Delta a_{\beta-H} = 3.46$ G, whereas for DMPO−O_2H they are $\Delta a_N = -0.11$ G and $\Delta a_{\beta-H} = 7.02$ G.[65] [b] Predicted isotropic hyperfine coupling constants for γ-H's with less than 1 G are not included in the table. [c] The hfsc differences $\Delta a_{x,gas}$ (defined as $a_{exptl} - a_{calcd,gas}$) in the gas phase for DMPO−OH are $\Delta a_{N,gas} = 3.31$ G and $\Delta a_{\beta-H,gas} = 8.83$ G, whereas for DMPO−O_2H they are $\Delta a_{N,gas} = 2.43$ G and $\Delta a_{\beta-H,gas} = 5.1$ G. In the aqueous phase, the Δa_x,a_q (defined as $a_{exptl} - a_{calcd,aq}$) for DMPO−OH are $\Delta a_{N,aq} = 2.11$ G and $\Delta a_{\beta-H,aq} = 5.38$ G, whereas for DMPO−O_2H they are $\Delta a_{N,aq} = 2.54$ G and $\Delta a_{\beta-H,aq} = -1.97$ G. [d] With DMPO−H adduct contamination (2−3%).

mixture did not give any indication for the presence of an amine functionality using ninhydrin reagent. Subjecting L-proline or pyrrolidine solutions, however, to the same spin-trapping conditions as with DMPO in the presence of similar concentrations of Na_2CO_3 and H_2O_2 showed positive results for an amine as evidenced by a yellow color upon ninhydrin treatment. These negative results for the DMPH−OCO_2^- formation may be due to the endoergic nature of the H-atom abstraction (reaction D) with $\Delta G_{298K,aq} = 24.9$ kcal/mol.

In order to establish the final form of the DMPO−CO_2 adduct in solution, the protonated form, DMPO−CO_2H, was theoretically optimized (Figure 3). According to Figure 3, the most preferred conformation in solution for DMPO−CO_2H is the cis conformation; however, the trans conformation is preferred in the gas phase. The $C_{CO2}-C_{ring}$ bond distances for both the cis and trans isomers are shorter (1.53−1.55 Å) compared to the unprotonated adduct with $C_{CO2}-C_{ring}$ bond distances of 1.60 Å. The acidity of DMPO−CO_2 adduct was then approximated based on our previous work,[65] according to the relationship

$$pK_a = 0.538(\Delta G_{aq,AH}) - 136.9$$

derived from all compounds listed in Table S2 of the Supporting Information. The pK_a of DMPO−CO_2H was predicted to be 6.4, whereas the measured pH was 6.8, thereby suggesting almost equal concentrations of both the DMPO−CO_2 adduct and DMPO−CO_2H in solution (Scheme 3).

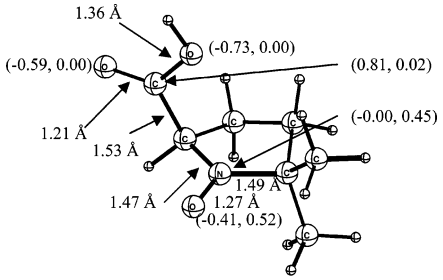

1.9 (-2.9)
DMPO-CO_2H-cis

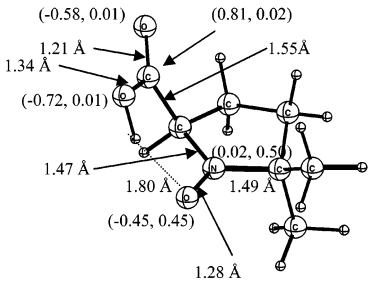

0.0 (0.0)
DMPO-CO_2H-trans

Figure 3. Bond distances, charge, and spin density population (in parentheses) of $CO_2^{\bullet-}$ adduct of DMPO in their protonated forms at the B3LYP/6-31+G**//B3LYP/6-31G* level as well as relative gas and aqueous (in parentheses) phase free energies (ΔG_{298K} in kcal/mol).

SCHEME 3

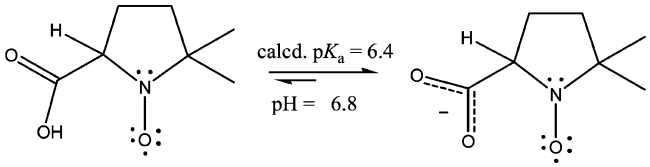

Conclusions

Theoretical as well as experimental evidence shows that $CO_2^{\bullet-}$ forms a C-centered adduct with DMPO. The mode of radical addition to DMPO is governed mostly by the spin population on the reacting radical, whereas charge characteristics of the radical only play a minor role in determining the type of adduct formed. Various modes of $CO_2^{\bullet-}$ addition to DMPO in solution were predicted that can result in the formation of various species such as (1) formation of a carboxylate adduct; (2) aminyl radical, in which thus far, our study shows the first theoretical evidence for the formation of aminyl radicals from a nitroxide, and (3) DMPO−OH. Although the formation of the aminyl radical is the most thermodynamically favored in solution but perhaps due to its high reactivity, only the carboxylate adduct was experimentally observed by EPR spectroscopy. The favorability of $CO_2^{\bullet-}$ ($\Delta G_{298K,aq} = -12.1$ kcal/mol) addition to DMPO is similar to that reported for mercapto ($^{\bullet}$SH) ($\Delta G_{298K,aq} = -12.8$ kcal/mol) radical addition to DMPO[63] suggesting that $CO_2^{\bullet-}$ formation in vivo can have biological significance and therefore consequences for oxidative damage.

Acknowledgment. This work was supported by NIH Grants HL38324, HL63744, and HL65608. C.M.H. acknowledges support from the NSF-funded Environmental Molecular Science Institute (CHE-0089147). A.R. acknowledges the Hungarian Scientific Research Fund Grant OTKA T-046953. The authors thank Prof. DeLanson R. Crist for helpful suggestions. The Ohio

Supercomputer Center (OSC) is acknowledged for generous computational support of this research.

Supporting Information Available: Energies, enthalpies, and free energies for all spin traps and their corresponding spin adducts. This information is available free of charge at http://pubs.acs.org.

References and Notes

(1) Halliwell, B. *Oxidative Stress Dis.* **2001**, *7*, 1.
(2) Halliwell, B. *Drugs Aging* **2001**, *18*, 685.
(3) Zweier, J. L.; Talukder, M. A. H. *Cardiovasc. Res.* **2006**, *70*, 181.
(4) Zweier, J. L.; Villamena, F. A. Chemistry of free radicals in biological systems. In *Oxidative Stress and Cardiac Failure*; Kukin, M. L., Fuster, V., Eds.; Futura Publishing: Armonk, N.Y., 2003; pp 67.
(5) Zweier, J. L.; Kuppusamy, P.; Lutty, G. A. *Proc. Natl. Acad. Sci. U.S.A.* **1988**, *85*, 4046.
(6) Zweier, J. L.; Kuppusamy, P.; Williams, R.; Rayburn, B. K.; Smith, D.; Weisfeldt, M. L.; Flaherty, J. T. *J. Biol. Chem.* **1989**, *264*, 18890.
(7) Stolze, K.; Udilova, N.; Nohl, H. *J. Biol. Chem.* **2002**, *383*, 813.
(8) Karoui, H.; Hogg, N.; Frejaville, C.; Tordo, P.; Kalyanaraman, B. *J. Biol. Chem.* **1996**, *271*, 6000.
(9) Olive, G.; Mercier, A.; Le Moigne, F.; Rockenbauer, A.; Tordo, P. *Free Radical Biol. Med.* **2000**, *28*, 403.
(10) Rosen, G. M.; Britigan, B. E.; Halpern, H. J.; Pou, S. *Free Radicals: Biology and Detection by Spin Trapping*; Oxford University Press: New York, 1999.
(11) Villamena, F.; Zweier, J. *J. Chem. Soc. Perkin Trans. 2* **2002**, 1340.
(12) Gianni, L.; Zweier, J.; Levy, A.; Myers, C. E. *J. Biol. Chem.* **1985**, *260*, 68206.
(13) Czapski, G.; Lymar, S. V.; Schwarz, H. A. *J. Phys. Chem. A* **1999**, *103*, 3447.
(14) Villamena, F. A.; Hadad, C. M.; Zweier, J. L. *J. Am. Chem. Soc.* **2004**, *126*, 1816.
(15) Zweier, J. L.; Flaherty, J. T.; Weisfeldt, M. L. *Proc. Natl. Acad. U.S.A.* **1987**, *84*, 1404.
(16) Zweier, J. L.; Kuppusamy, P.; Lutty, G. A. *Proc. Natl. Acad. U.S.A.* **1988**, *85*, 4046.
(17) Zweier, J. L.; Kuppusamy, P.; Williams, R.; Rayburn, B. K.; Smith, D.; Weisfeldt, M. L.; Flaherty, J. T. *J. Biol. Chem.* **1989**, *264*, 18890.
(18) Wang, P.; Chen, H.; Qin, H.; Sankarapandi, S.; Becher, M. W.; Wong, P. C.; Zweier, J. L. *Proc. Natl. Acad. Sci. U S A* **1998**, *95*, 4556.
(19) Villamena, F. A.; Zweier, J. L. *Antioxid. Redox Signaling* **2004**, *6*, 619.
(20) Dikalova, A. E.; Kadiiska, M. B.; Mason, R. P. *Proc. Natl. Acad. Sci. U.S.A.* **2001**, *98*, 13549.
(21) LaCagnin, L. B.; Connor, H. D.; Mason, R. P.; Thurman, R. G. *Mol. Pharmacol.* **1988**, *33*, 351.
(22) Rau, J. M.; Reinke, L. A.; McCay, P. B. *Free Radic. Res. Commun.* **1990**, *9*, 197.
(23) Taniguchi, H.; Madden, K. P. *Radiat. Res.* **2000**, *153*, 447.
(24) Barbati, S.; Clement, J. L.; Olive, G.; Roubaud, V.; Tuccio, B.; Tordo, P. ^{13}P labeled cyclic nitrones: A new class of spin traps for free radicals in biological milieu. In *Free Radicals in Biology, Environment*; Minisci, F., Ed.; Kluwer Academic Publishers: Dordrecht, The Netherlands, 1997; pp 39.
(25) Kochany, J.; Lipczynska-Kochany, E. *Chemosphere* **1992**, *25*, 1769.
(26) Yoon, J. H.; Jung, J.; Chung, H. H.; Lee, M. J. *J. Radioanal. Nucl. Chem.* **2002**, *253*, 217.
(27) Neta, P.; Huie, R. E.; Ross, A. B. *J. Phys. Chem. Ref. Data* **1988**, *17*, 1027.
(28) Labanowski, J. W.; Andzelm, J. *Density Functional Methods in Chemistry*; Springer: New York, 1991.
(29) Parr, R. G.; Yang, W. *Density Functional Theory in Atoms and Molecules*; Oxford University Press: New York, 1989.
(30) Becke, A. D. *Phys. Rev.* **1988**, *38*, 3098.
(31) Lee, C.; Yang, W.; Parr, R. G. *Phys. Rev. B* **1988**, *37*, 785.
(32) Becke, A. D. *J. Chem. Phys.* **1993**, *98*, 1372.
(33) Hehre, W. J.; Radom, L.; Schleyer, P. V.; Pople, J. A. *Ab Initio Molecular Orbital Theory*; John Wiley & Sons: New York, 1986.
(34) Tomasi, J.; Persico, M. *Chem. Rev.* **1994**, *94*, 2027.
(35) Cossi, M.; Barone, V.; Cammi, R.; Tomasi, J. *Chem. Phys. Lett.* **1996**, *255*, 327.
(36) Barone, V.; Cossi, M.; Tomasi, J. *J. Chem. Phys.* **1997**, *107*, 3210.
(37) Barone, V.; Bencini, A.; Cossi, M.; Di Matteo, A.; Mattesini, M.; Totti, F. *J. Am. Chem. Soc.* **1998**, *120*, 7069.
(38) Tomasi, J.; Mennucci, B.; Cammi, R. *Chem. Rev.* **2005**, *105*, 2999.
(39) Frisch, M. J.; et al. Gaussian 03, revision B.04; Gaussian, Inc.: Pittsburgh PA, 2003.
(40) Reed, A. E.; Curtiss, L. A.; Weinhold, F. A. *Chem. Rev.* **1988**, *88*, 899.
(41) Scott, A. P.; Radom, L. *J. Phys. Chem.* **1996**, *100*, 16502.
(42) Barone, V.; Bencini, A.; Cossi, M.; Di Matteo, A.; Mattesini, M.; Totti, F. *J. Am. Chem. Soc.* **1998**, *120*, 7069.
(43) Cirujeda, J.; Vidal-Gancedo, J.; Jurgens, O.; Mota, F.; Novoa, J. J.; Rovira, C.; Veciana, J. *J. Am. Chem. Soc.* **2000**, *122*, 11393.
(44) Pavone, M.; Cimino, P.; De Angelis, F.; Barone, V. *J. Am. Chem. Soc.* **2006**, *128*, 4338.
(45) Saracino, G. A. A.; Tedeschi, A.; D'Errico, G.; Improta, R.; Franco, L.; Ruzzi, M.; Corvaia, C.; Barone, V. *J. Phys. Chem. A* **2002**, *106*.
(46) Barone, V. In *Recent Advances in Density Functional Theory, Part 1*; Cong, D. P., Ed.; World Scientific Publishing Co.: Singapore, 1995; pp 287.
(47) Woon, D. E.; Dunning, T. H. *J. Chem. Phys.* **1995**, *103*, 4572.
(48) Villamena, F. A.; Merle, J. K.; Hadad, C. M.; Zweier, J. L. *J. Phys. Chem. A* **2005**, *109*, 6089.
(49) Rockenbauer, A.; Korecz, L. *Appl. Magn. Reson.* **1996**, *10*, 29.
(50) Gordon, A. J.; Ford, R. A. *The Chemist's Companion: A Handbook of Practical Data, Techniques, and References*; Wiley-Interscience: New York, 1972.
(51) Boeyens, J. C. A.; Kruger, G. J. *Acta Cryst.* **1970**, *B26*, 668.
(52) Villamena, F.; Dickman, M. H.; Crist, D. R. *Inorg. Chem.* **1998**, *37*, 1446.
(53) Villamena, F. A.; Rockenbauer, A.; Gallucci, J.; Velayutham, M.; Hadad, C. M.; Zweier, J. L. *J. Org. Chem.* **2004**, *69*, 7994.
(54) Huanga, W.; Qianb, H.; Goua, S.; Yaob, C. *J. Mol. Struct.* **2005**, *743*, 183.
(55) Djordjevic, C.; Vuletic, N.; Jacobs, B. A.; Lee-Renslo, M.; Sinn, E. *Inorg. Chem.* **1997**, *36*, 1798.
(56) Kaim, W. *Science* **2005**, *307*, 216.
(57) Alsfassi, Z. In *N-Centered Radicals*; Maxwell, J. T., Ed.; Wiley: New York, 1998; pp 663.
(58) Stubbe, J.; van der Donk, W. A. *Chem. Rev.* **1998**, *98*, 705.
(59) Armstrong, D. A.; Asmus, K.-D.; Bonifacic, M. *J. Phys. Chem. A* **2004**, *108*, 2238.
(60) Lalevee, J.; Allonas, X.; Fouassier, J.-P. *J. Am. Chem. Soc.* **2002**, *124*, 9613.
(61) Bonifacic, M.; Armstrong, D. A.; Carmichael, I.; Asmus, K.-D. *J. Phys. Chem. B* **2000**, *104*, 643.
(62) Buettner, T.; Geier, J.; Frison, G.; Harmer, J.; Calle, C.; Schweiger, A.; Schoenberg, H.; Gruetzmacher, H. *Science* **2005**, *307*, 235.
(63) Villamena, F. A.; Hadad, C. M.; Zweier, J. L. *J. Phys. Chem. A* **2005**, *109*, 1662.
(64) Villamena, F.; Hadad, C. M.; Zweier, J. L. *J. Phys. Chem. A* **2003**, *107*, 4407.
(65) Villamena, F. A.; Merle, J. K.; Hadad, C. M.; Zweier, J. L. *J. Phys. Chem. A.* **2005**, *109*, 6089.